Localized zones of Rho and Rac activities drive initiation and expansion of epithelial cell–cell adhesion

Soichiro Yamada[1] and W. James Nelson[1,2]

[1]Department of Molecular and Cellular Physiology and [2]Department of Biological Sciences, Stanford University, Stanford, CA 94305

Spatiotemporal coordination of cell–cell adhesion involving lamellipodial interactions, cadherin engagement, and the lateral expansion of the contact is poorly understood. Using high-resolution live-cell imaging, biosensors, and small molecule inhibitors, we investigate how Rac1 and RhoA regulate actin dynamics during de novo contact formation between pairs of epithelial cells. Active Rac1, the Arp2/3 complex, and lamellipodia are initially localized to de novo contacts but rapidly diminish as E-cadherin accumulates; further rounds of activation and down-regulation of Rac1 and Arp2/3 occur at the contacting membrane periphery, and this cycle repeats as a restricted membrane zone that moves outward with the expanding contact. The cortical bundle of actin filaments dissolves beneath the expanding contacts, leaving actin bundles at the contact edges. RhoA and actomyosin contractility are activated at the contact edges and are required to drive expansion and completion of cell–cell adhesion. We show that zones of Rac1 and lamellipodia activity and of RhoA and actomyosin contractility are restricted to the periphery of contacting membranes and together drive initiation, expansion, and completion of cell–cell adhesion.

Introduction

Cell–cell adhesion is a fundamental feature of multicellular organisms and is involved in all aspects of tissue morphogenesis. In particular, cadherin-mediated cell–cell adhesion plays important roles in determining cell shape, movement, and sorting (Takeichi, 1995; Gumbiner, 2005), for example, during embryo compaction (Vestweber and Kemler, 1985; Larue et al., 1994), gastrulation (Lee and Gumbiner, 1995; Costa et al., 1998), and packing of photoreceptors in the retinal epithelium (Hayashi and Carthew, 2004). In addition to dynamic changes in the organization of cell–cell contacts, these complex cell movements require remodeling of the actin cytoskeletal network to effect global changes in cell shape. One of the keys to understanding tissue morphogenesis is to determine the interplay between cell–cell adhesion and activation of mechanical forces that control membrane dynamics and cell shape.

Correspondence to W. James Nelson: wjnelson@stanford.edu

S. Yamada's present address is Department of Biomedical Engineering, Genome and Biomedical Sciences Facility, University of California, Davis, Davis, CA 95616.

Abbreviations used in this paper: CD, cytochalasin D; FRET, fluorescence resonance energy transfer; MLCK, myosin light chain kinase; ROCK, Rho kinase; TIRF-M, total internal reflection fluorescence microscopy.

The online version of this article contains supplemental material.

Initial contacts between cells involve interactions between opposing lamellipodia that initiate E-cadherin clustering and the subsequent expansion of the contact to form strong cell–cell adhesion (Adams et al., 1998; Krendel and Bonder, 1999; Ehrlich et al., 2002; Vaezi et al., 2002). These dynamic processes indicate diverse roles for the actin cytoskeleton in cell–cell adhesion. Lamellipodia activity is mediated by Rac1-controlled actin dynamics. Rac1 is activated upon E-cadherin adhesion (Braga et al., 1997; Nakagawa et al., 2001; Noren et al., 2001), and Rac1 protein localizes with E-cadherin during cell–cell adhesion (Nakagawa et al., 2001; Ehrlich et al., 2002). However, the localization and dynamic regulation of Rac1 activity during cell–cell adhesion has not been followed, nor has the distribution of Rac1 activity been compared with the distribution and activities of its downstream effectors, the Arp2/3 complex and lamellipodia. It is generally thought that Rac1 activation induces interactions between the cortical actin cytoskeleton and cadherins, but recent studies testing binding of actin to the cadherin–catenin complex revealed that the interaction is not direct (Drees et al., 2005; Yamada et al., 2005). In light of these results, actin dynamics may be involved in other aspects of cell–cell adhesion, and therefore, the organization of actin during cell–cell adhesion needs to be reexamined.

Supplemental material can be found at:
http://doi.org/10.1083/jcb.200701058

The Journal of Cell Biology, Vol. 178, No. 3, July 30, 2007 517–527
http://www.jcb.org/cgi/doi/10.1083/jcb.200701058

Contraction of actin filaments by nonmuscle myosin II has been suggested to play a role during cell–cell adhesion in embryonic development (Bertet et al., 2004; Conti et al., 2004; Zallen and Wieschaus, 2004; Dawes-Hoang et al., 2005), stratification of keratinocytes (Vaezi et al., 2002; Zhang et al., 2005), and assembly of cell–cell junctions in epithelial monolayers (Krendel and Bonder, 1999; Ivanov et al., 2004; Ivanov et al., 2005; Shewan et al., 2005). It is thought that activated myosin II generates contractile forces at the cell periphery that expand or constrict cell shape during morphogenetic cell movements (Bertet et al., 2004). However, it is unclear how or where myosin II and contractile forces are locally activated and generated. Previous studies focused on the effects of disruption of actomyosin contraction on E-cadherin distribution and analysis of fixed cells (Krendel and Bonder, 1999), cell–cell adhesion within confluent cell monolayers upon removal or readdition of extracellular Ca^{2+} (Vaezi et al., 2002; Ivanov et al., 2004, 2005; Zhang et al., 2005), or artificial spreading of cells on an E-cadherin substrate (Shewan et al., 2005). None of these studies, however, identified mechanisms regulating activation and location of, or the mechanical forces produced by, the actomyosin contractile apparatus during de novo cell–cell adhesion.

Here, we studied mechanisms coordinating different stages of de novo cell–cell adhesion between pairs of normal epithelial (MDCK) cells. Using high-resolution live-cell imaging, biosensors, and small molecule inhibitors, we show for the first time that Rac1 and RhoA activities and their downstream effectors are restricted to zones at the edges of the expanding contact and that rounds of activation and down-regulation of these GTPases are involved in the initiation, expansion, and completion of cell–cell adhesion.

Results

Reorganization of E-cadherin and actin during de novo cell–cell adhesion

High-resolution live-cell imaging of GFP-labeled E-cadherin (E-cadherin–GFP) in MDCK cells revealed that initial adhesion was established by extension of, and contact between, lamellipodia from opposing plasma membranes that resulted in local accumulations of E-cadherin–GFP at those sites. Subsequently, the overall level of E-cadherin–GFP at cell–cell contacts gradually increased as the contact began to expand (Fig. 1, A and B), but during the latter stages of cell–cell adhesion, much of the E-cadherin–GFP moved to the edges of cell–cell contact with relatively less remaining in the middle of the contact (see kymograph [Fig. 1 A] and intensity profile [Fig. 1 B] along the cell–cell contact; Video 1, available at http://www.jcb.org/cgi/content/full/jcb.200701058/DC1; Adams et al., 1998). The process of cell–cell adhesion was rapid (0.89 ± 0.15 μm/min), and the cell–cell contact maximized to a final length (40.3 ± 1.9 μm), similar to that of the cell diameter (Fig. 1, C–E). These results reveal two distinct stages of E-cadherin organization during de novo cell–cell adhesion formation and the role of active membrane processes in each stage: first, E-cadherin accumulation induced by contacts between opposing lamellipodia, and second, reorganization of E-cadherin to the periphery as the contact expanded.

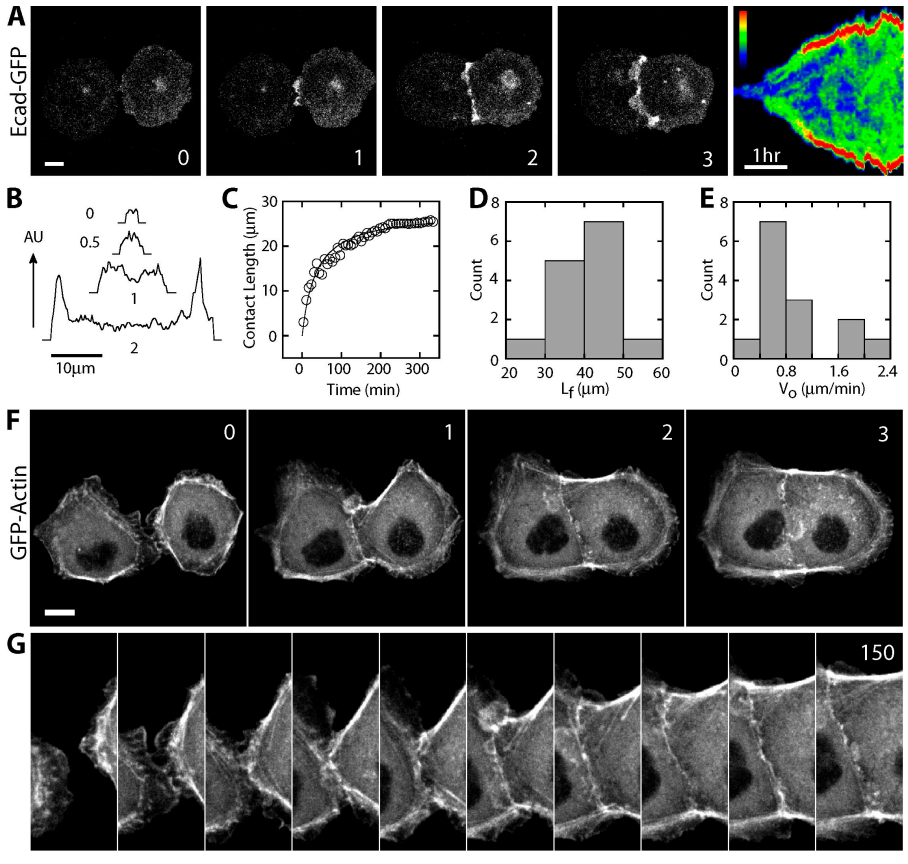

Figure 1. **Dynamics of E-cadherin and actin during expansion of de novo epithelial cell–cell adhesions.** (A) Formation of cell–cell contacts between two E-cadherin–GFP–expressing MDCK cells. The last panel is a kymograph of pseudocolored intensity scans along the cell–cell contact. (B) E-cadherin–GFP intensity profile along the cell–cell contact at 0, 0.5, 1, and 2 h after the initial contact. (C) Quantification of cell–cell contact length shown in A and B. For each frame, the cell–cell contact was manually traced and the length was quantified (circles). The solid line is a fitted curve. (D) Distributions of final cell–cell contact lengths, L_f, measured from 14 different cell–cell contacts. (E) Initial velocities of cell–cell contact formation, v_o, measured from 14 different cell–cell contacts. (F and G) Formation of cell–cell contacts between two MDCK cells expressing GFP-actin. Numbers indicate time in hours (A, B, and F) or minutes (G). Bars, 10 μm.

Next, we examined the distribution of GFP-actin to determine whether changes in actin organization coincided with these two stages of E-cadherin reorganization during cell–cell adhesion. In individual cells, in the absence of cell–cell contact, actin filaments formed a thick cortical bundle that circumscribed the cell periphery and a more diffuse organization in extending lamellipodia (Fig. 1 F and Video 2, available at http://www.jcb.org/cgi/content/full/jcb.200701058/DC1). During the initial stages of cell–cell adhesion, the cortical actin bundle appeared to disassemble in the immediate vicinity of the contact (Ehrlich et al., 2002), leaving a gap between the ends of the actin bundle that became wider as the contact expanded. This gap in the cortical actin bundle colocalized with accumulated E-cadherin (Fig. 1, F and G). Some diffuse actin remained at the cell–cell contact, but it was mostly associated with lamellipodia that intermittently swept over parts of the contact and particularly at the edges as the contact expanded laterally. Thus, both actin and E-cadherin undergo dramatic reorganization during the initial stage of adhesion and subsequent expansion of the contact, but their distributions are different: E-cadherin accumulates in a zone that expands outwards as the contact grows, whereas actin filaments are prominent at the edges of the expanding E-cadherin zone and are greatly reduced within the contact itself.

The ends of the actin bundle are highly dynamic and contractile

To examine mechanisms involved in the reorganization of the actin network during cell–cell adhesion, we identified sites of actin contractility and dynamic assembly. We used low concentrations of cytochalasin D (CD; 0.5 μM) to cap the barbed ends of actin filaments and examined effects on the actin network during cell–cell adhesion in live cells (Fig. 2, A–D); our goals were to see if the barbed ends of actin filaments were displaced from putative anchorage points on the membrane and to examine the consequences on the cortical bundle.

After CD addition, small actin asters appeared along and at the ends of the cortical actin bundle. Interestingly, actin asters did not form immediately adjacent to the contact itself (Fig. 2 A and Video 3, available at http://www.jcb.org/cgi/content/full/jcb.200701058/DC1), supporting our earlier observation that the actin bundle disassembles immediately beneath the expanding

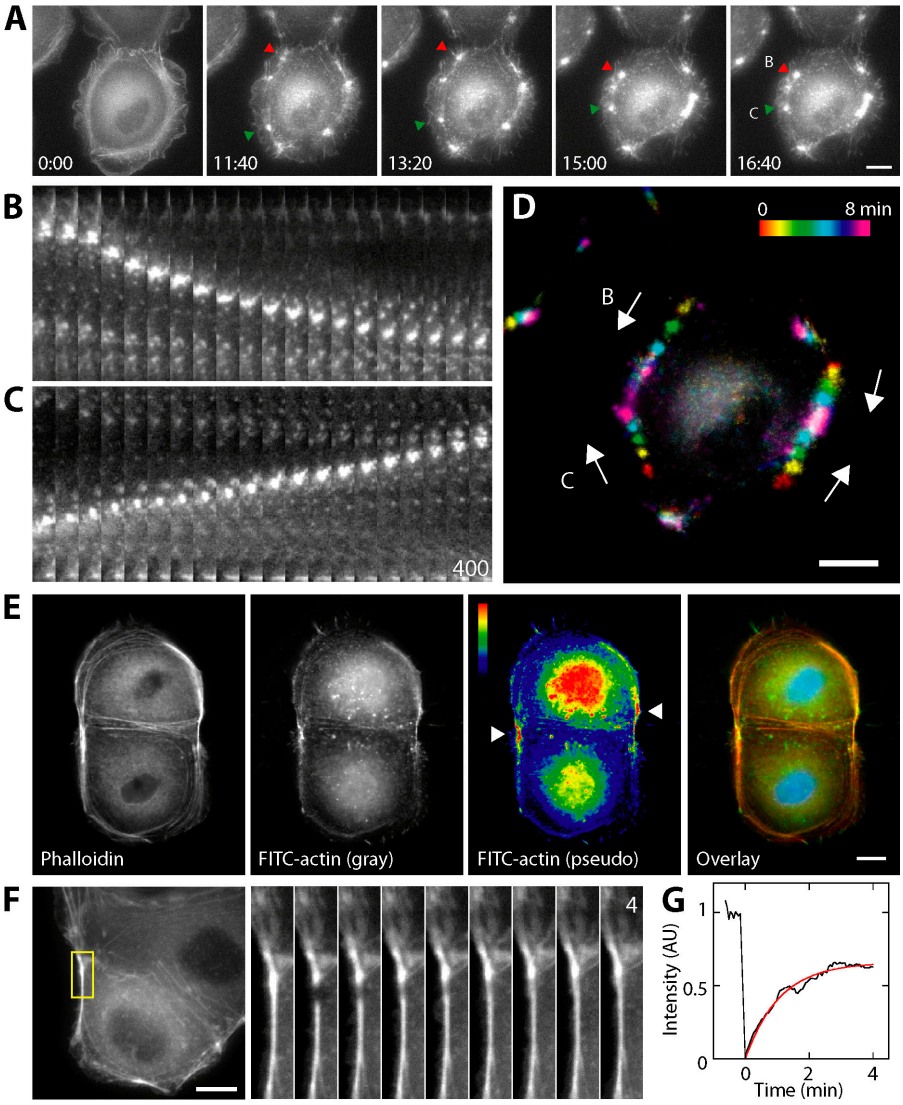

Figure 2. **Contraction and polymerization of the cortical actin bundle.** (A) 0.5 μM CD–treated MDCK cells expressing GFP-actin. Movements of two GFP-actin asters are indicated by red and green arrowheads. Time is in min:s. (B and C) Montages of images of actin asters along the cortical actin bundle. (D) Pseudocolored maximal projection of images shown in A; pseudocolors represent different time points as indicated, and arrows point in the directions of aster motion. (E) FITC-actin incorporation in saponin-permeabilized cells. FITC-actin staining is shown as in gray or a pseudocolored scale. The overlay image is generated from pseudocolored phalloidin (red), FITC-actin (green), and DAPI (blue) staining. (F) FRAP of GFP-actin bundles near a cell–cell junction. (G) Fluorescence recovery profile of data in F. Bars, 10 μm.

cell–cell contact. Actin asters are thought to be generated by tension in the actin network through nonmuscle myosin II (Verkhovsky et al., 1997) and therefore provide fiduciary marks for changes in actin organization brought about by the release of tension in the cortical actin bundle. We observed that actin asters translocated away from the edges of the cell–cell contact along the remaining cortical bundle (Video 3); we interpret this movement as a consequence of the release of CD-capped barbed ends of actin filaments from anchorage points at the edges of the cell–cell contact. We also observed two distinct groups of actin asters, one from each edge of the cell–cell contact and the other from the opposite noncontacting end of the cell, presumably at the sites of focal adhesions, which translocated toward each other with a mean speed of 1.26 ± 0.3 μm/min (Fig. 2, A–D); we interpret this movement as evidence of the direction of contractile forces in the cortical bundle away from the edges of the cell–cell contact. Together, these results indicate that (1) there is little or no actin tension along the cell–cell contact itself; (2) the cortical actin bundle is under global tension around the cell perimeter; and (3) anchorage points for the barbed end of actin filaments appear to be located at the edges of the expanding cell–cell contact and at the opposite, noncontacting end of cells.

To examine whether actin filament assembly occurred at the barbed ends located at the edges of cell–cell contacts as indicated from the CD experiment, we measured G-actin incorporation and actin turnover. In saponin-permeabilized cells, FITC-labeled G-actin preferentially incorporated into cortical actin structures at the edges of cell–cell contacts and some focal contacts close to the substratum (Fig. 2 E); note that there was little or no FITC-labeled G-actin incorporation along the cell–cell contact where E-cadherin had accumulated.

We examined actin turnover using FRAP. Localized photobleaching of GFP-actin in cortical actin bundles at the edges of a compacted contact revealed that actin was highly dynamic ($\tau_{1/2}$ = ~1 min; Fig. 2, F and G; and Video 4, available at http://www.jcb.org/cgi/content/full/jcb.200701058/DC1), consistent with the high level of actin polymerization at those sites shown by FITC-actin incorporation (Fig. 2 E). Actin in cortical bundles in single cells or at the noncontacting sides of adhering cells also exhibited a turnover rate similar to that shown at the edges of cell–cell contacts (unpublished data). However, in contrast to the edges of cell–cell contacts, we detected little or no FITC-actin incorporation in cortical bundles at free, noncontacting edges (Fig. 2 E), indicating that barbed-end actin polymerization is

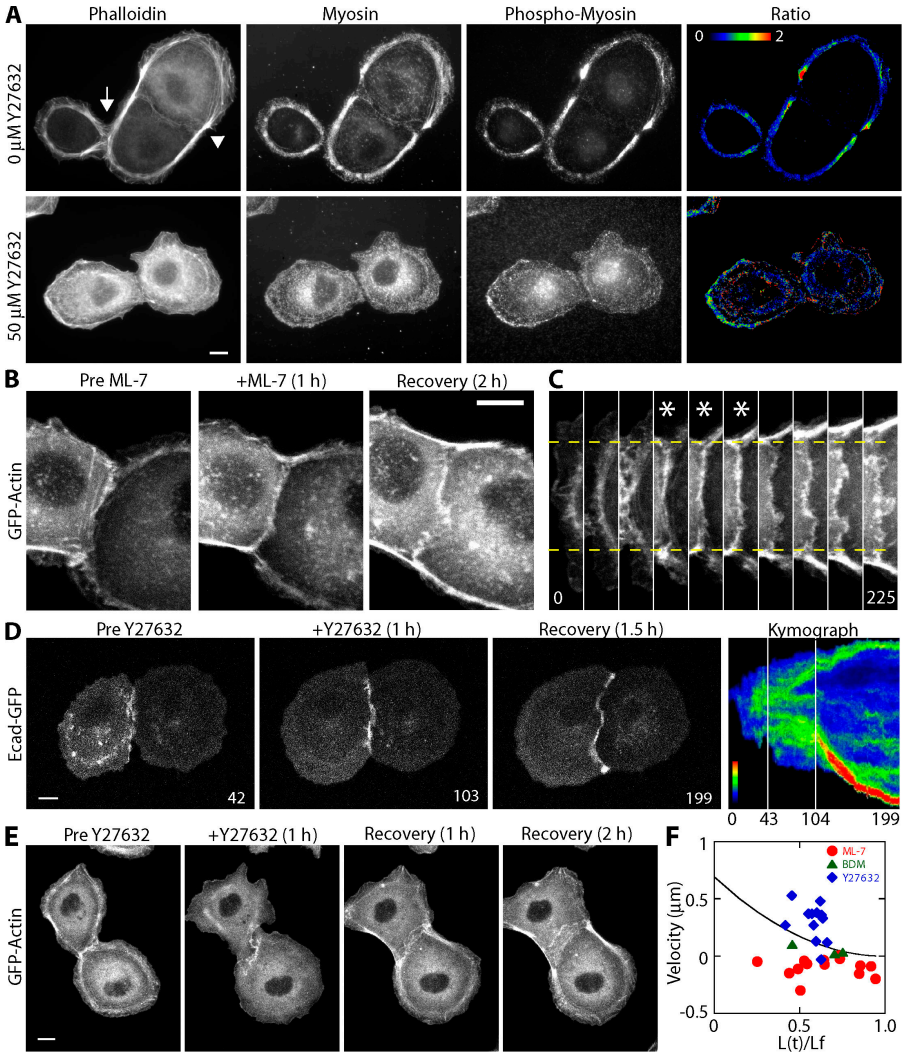

Figure 3. **Actin-myosin contraction drives contact expansion.** (A) Immunostaining of phalloidin, myosin II, and phosphomyosin II. Arrowhead indicates the edges of a mature cell–cell contact, and arrow indicates a nascent cell–cell contact. The ratio images are pseudocolored based on a pixel-to-pixel ratio of phosphomyosin II and total myosin II. (B) GFP-actin–expressing MDCK cells before, during, and after 25 μM ML-7 addition. (C) Montages of images of the cell–cell contact shown in B; asterisk indicates the time of ML-7 addition. (D) E-cadherin–GFP–expressing MDCK cells before, during, and after 50 μM Y27632 addition; the last panel is a kymograph of pseudocolored intensity scans along the cell–cell contact. (E) GFP-actin–expressing MDCK cells before, during, and after 50 μM Y27632 addition. (F) Expansion velocities of cell–cell contacts during ML-7, Y27632, and BDM treatments. The velocities were calculated by dividing the change in the contact length by duration of drug treatment, and plotted as a function of normalized contact length (L[t]/Lf, where L[t] is contact length and Lf is final contact length). As the expansion velocity depends on the maturation of cell–cell contact (Fig. 1 C), the mean velocity profile from Fig. 1 (D and E) is plotted as a reference (line). 25 mM BDM had no effect on the velocity. Bars, 10 μm.

not the mechanism for observed actin turnover at those sites. Collectively, these results indicate that the cortical actin bundle is under global tension and undergoing polymerization at the barbed ends of filaments localized to the edges of the expanding cell–cell contact.

Activated myosin II drives cell–cell contact formation

The results thus far indicate that the cortical actin bundle is generating mechanical forces from anchorage points at the edges of the cell–cell contact. Contraction of cortical actin bundle is mediated by nonmuscle myosin II; therefore, we examined the distribution of activated myosin II in adhering MDCK cell pairs. We found that total myosin II localized along cell–cell contacts, as reported previously (Krendel et al., 1999; Ivanov et al., 2005; Shewan et al., 2005; Zhang et al., 2005), and throughout the cortical actin bundle (Fig. 3 A; Krendel and Bonder, 1999). Using a phosphospecific (S19) myosin II antibody (Matsumura et al., 1998) to detect activated myosin II, we found that the highest levels of activated myosin II were concentrated in the ends of the cortical actin bundle located at the edges of expanding cell–cell contacts. Lesser amounts of phosphomyosin II were also located throughout the rest of the cortical bundle (Fig. 3 A, arrowhead), but little or none was detected within the cell–cell contact (Fig. 3 A). Even at the earliest stage of cell–cell contact (Fig. 3 A, arrow), we found that activated myosin II was preferentially localized at the edges of the expanding contact and excluded from the cell–cell contact itself.

Activation of actomyosin contractility requires phosphorylation of myosin light chains by Rho kinase (ROCK) and myosin light chain kinase (MLCK). Inhibition of ROCK by Y27632 resulted in less organized and more diffuse cortical actin bundle and inhibited the localization of activated myosin II at the edges of the cell–cell contact, although some diffuse phosphomyosin II staining was detected throughout the cell (Fig. 3 A). These results indicate that ROCK activity is required to both localize and activate myosin II to the edges of cell–cell contacts. Note that ROCK inhibition did not dissociate the cell–cell contact, indicating that the maintenance of cell–cell adhesion does not require activated myosin II and actomyosin contractility; this is also consistent with the lack of phosphomyosin II staining within the cell–cell contact (Fig. 3 A).

To determine roles of activated myosin II during completion of cell–cell contacts, we examined the effects of introducing the small molecule inhibitors ML-7, a MLCK inhibitor, and Y27632 into live cells. Addition of 25 μM ML-7 to MDCK cells expressing GFP-actin caused the immediate seizure of cell–cell contact expansion (Fig. 3 B and Video 5, available at http://www.jcb.org/cgi/content/full/jcb.200701058/DC1), although prominent cortical GFP-actin bundles remained intact at the edges of the contact. Addition of ML-7 to newly established cell–cell contacts resulted in negative velocities of expansion because of retraction of lamellipodia and detachment of cell–cell contacts (Fig. 3 F; see Materials and methods for the measurements of expansion velocities).

Addition of 50 μM Y27632 had a lesser effect than ML-7 on the expansion of cell–cell contacts (Fig. 3 F). Although Y27632 inhibited myosin II activation (Fig. 3 A), it had little effect on lamellipodia activity, which appeared to be sufficient to induce additional contact formation and expansion but not compaction of the contact (Fig. 3, D–F). Note that in the presence of Y27632, E-cadherin–GFP remained along cell–cell contacts, but clusters did not form at edges of cell–cell contacts (Fig. 3 D and Video 6, available at http://www.jcb.org/cgi/content/full/jcb.200701058/DC1), indicating that activation of myosin II is required for this stage in E-cadherin reorganization. This was confirmed by Y27632 washout, which resulted in the reformation of large E-cadherin–GFP clusters and the rapid movement of those clusters to the edges of expanding cell–cell contact (Fig. 3 D and Video 6). Although cell–cell contact remained intact during Y27632 treatment, the cortical actin bundle completely disassembled (Fig. 3 E and Video 7). Washout of Y27632 resulted in the rapid reassembly of the cortical actin bundle, which was, as before addition of inhibitor, particularly prominent at the edges of the cell–cell contact. Similar morphological effects were observed with blebbistatin (unpublished data), but no live-cell fluorescence images were collected because of the phototoxicity of blebbistatin. These results indicate that activation of myosin II and organization of the cortical actin bundle are locally controlled at the edges of the contact by the activity of ROCK and MLCK and that activation of myosin II by MLCK and ROCK is required for completion of cell–cell contact.

Distributions of activated Rac1 and RhoA GTPases during cell–cell adhesion

Members of the Rho family of small GTPase have been implicated in myosin II–mediated contraction (RhoA), lamellipodia activity (Rac1; Etienne-Manneville and Hall, 2002), and cell–cell adhesion (Braga et al., 1997; Takaishi et al., 1997; Jou and Nelson, 1998; Nakagawa et al., 2001). During the formation of cell–cell contacts, we observed minimal filopodia activity and therefore did not focus on a role for Cdc42. Dominant-negative and constitutively active forms of Rho family small GTPases have been used to perturb the activities of endogenous proteins, but they do not show the distribution of GTPase activity and often cause pleiotropic effects on cell spreading and motility that interfere with the analysis of cell–cell adhesion. Therefore, we chose to use Raichu fluorescence resonance energy transfer (FRET)–based biosensors (Itoh et al., 2002; Yoshizaki et al., 2003) to follow the distributions of RhoA and Rac1 activities during compaction of cell–cell adhesion in live cells. These Raichu probes are chimeric proteins of Rac1 or RhoA and a Rho binding domain of an effector protein p21-activated kinase or protein kinase N, respectively. Upon activation by GTP loading, FRET efficiency increases as the result of an intramolecular conformational change. We chose to examine the distributions of active Rac1 and RhoA in adhering cell pairs in which only one of the cells expressed the Raichu probe, and therefore the fluorescence signal could be unequivocally localized; one representative example of each FRET pair from three to five independent experiments is shown.

Transient expression of Raichu-Rac1 in MDCK cells showed high FRET efficiency in active lamellipodia at the edges of the

expanding cell–cell contact (Fig. 4 A, arrows; and Video 8, available at http://www.jcb.org/cgi/content/full/jcb.200701058/DC1). Only the Raichu-positive cell is visible (Fig. 4 A, left; cell–cell contact is located at the middle of each panel). In general, Raichu-Rac1 FRET was absent from older areas of the cell–cell contact that had formed previously, although occasionally a lamellipodium would transiently form in the middle of the contact, and Raichu-Rac1 FRET was prominent at the leading edge of the membrane (Fig. 4 A, asterisk).

The high FRET efficiency of Raichu-Rac1 at the edges of the expanding contact coincided with protruding lamellipodia, where we had shown that actin turnover was also high (Fig. 2 F). Actin and membrane dynamics initiated upon Rac1 activity are mediated by localized activity of the Arp2/3 complex. We examined the distribution of the Arp2/3 complex using Arp3-GFP (Welch et al., 1997) during cell–cell adhesion (Fig. 4 B and Video 9, available at http://www.jcb.org/cgi/content/full/jcb.200701058/DC1). We found that during initiation of cell–cell adhesion, Arp3-GFP was localized at the tips of lamellipodia along the forming contact (Fig. 4 B, frames 1–5). Subsequently, as the cell–cell contact expanded, Arp3-GFP and lamellipodia were localized to the edges of the contact (Fig. 4 B, frame 8 and onward), with fewer incidences within the contact itself. The distributions of Arp3-GFP and lamellipodia at the edges of the expanding contact appear similar to that of active Rac1 (Fig. 4, compare A and B).

In migrating single MDCK cells, Raichu-RhoA FRET was highest around the leading edge and in the retracting uropod at the rear of the cell (Fig. 4 C), as previously described in fibroblasts (Pertz et al., 2006); these distributions are consistent with the role of RhoA in regulating actomyosin contraction at the edges of lamellipodia and in retraction of the plasma membrane during cell migration (Etienne-Manneville and Hall, 2002). During expansion of cell–cell contacts, Raichu-RhoA FRET was most prominent at the most distal edges of the expanding cell–cell contact but was absent along the cell–cell contact and at the tip of lamellipodia (Fig. 4 D and Video 10, available at http://www.jcb.org/cgi/content/full/jcb.200701058/DC1). Only the Raichu-positive cell is visible (Fig. 4 D, left; cell–cell contact is located at the middle of each panel). Note that membranes at the edge of cell–cell contact that had high RhoA FRET activity did not have dynamic lamellipodia-like membrane activity, like those with high Raichu-Rac1 FRET (Fig. 4 A), but instead exhibited persistent membrane growth. The distribution of highest RhoA FRET appeared similar to that of phosphomyosin II (compare Fig. 4 D with Fig. 3 A).

We are unable to directly compare Rac1 and RhoA FRET in the same cell. However, we note that Rac1 FRET localized to the tips of transient lamellipodia at the edges of the contact, whereas RhoA FRET was observed to persist at the sides of the most distal edges of the expanding contact (Fig. 4, compare A and D), indicating that the distributions are different and that active RhoA localized more at the outside of the contact than active Rac1.

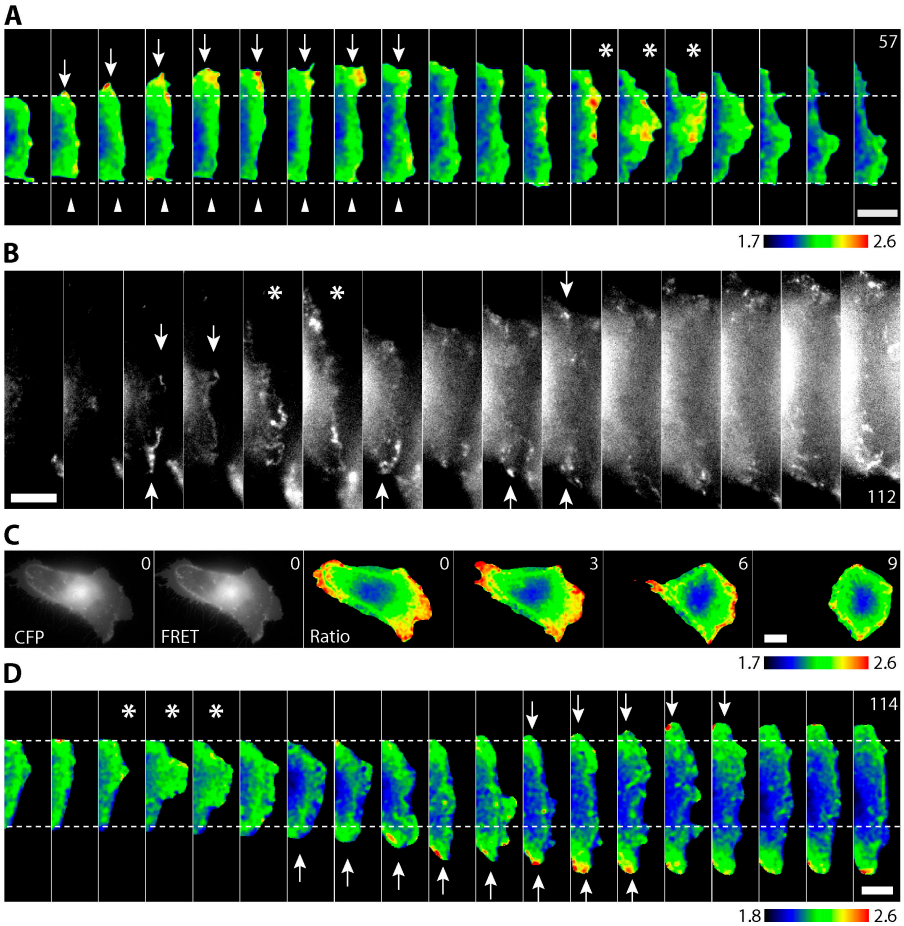

Figure 4. **Rac1 and RhoA activation during contact expansion.** (A) Raichu-Rac1–expressing MDCK cell making cell–cell contact with a nonexpressing MDCK cell. Arrows point to expanding edge of cell–cell contact, and arrowheads point to stationary cell–cell contact. Asterisks indicate Rac1-positive lamellipodium formation. (B) Arp3-GFP–expressing MDCK cells making cell–cell contacts. Arrows point to transient accumulation of Arp3-GFP at lamellipodia. Asterisks indicate lamellipodium formation along the cell–cell contact. (C) Raichu-RhoA–expressing MDCK cells. Raw CFP, FRET, and ratio images are shown of a migrating cell. (D) Raichu-RhoA–expressing MDCK cell making cell–cell contact with a nonexpressing MDCK cell. Arrows point to expanding edge of cell–cell contact, and asterisks indicate RhoA-negative lamellipodium formation. Time is in minutes. Bars, 10 μm.

Mechanisms regulating local RhoA activation

Our results show that RhoA and its downstream effectors ROCK and MLCK are locally active at the edge of cell–cell contacts and are critical for expansion of contacts, but the question is, how is RhoA specifically activated at that site on the plasma membrane? One pathway that activates RhoA is integrin-mediated adhesion and clustering (Ren et al., 1999); it is interesting to note that integrin-mediated adhesion also regulates cadherin function during embryonic development and epithelial–mesenchymal transitions (Chen and Gumbiner, 2006). To explore possible cross talk between these two adhesion systems, we examined the spatial proximity of sites of E-cadherin–mediated adhesion to the basal cell surface, where integrin-mediated adhesion to the substratum occurs. Using total internal reflection fluorescence microscopy (TIRF-M) in live cells, we detected E-cadherin–GFP clusters at the edges of fully expanded cell–cell contacts that were in close proximity to the substratum (Fig. 5 A, arrowheads). By TIRF-M, E-cadherin–GFP in the middle of the cell–cell contact was only detectable at the early stage of cell–cell contact (Fig. 5 A, arrows), but not at the later stage and was only visible using widefield fluorescence microscopy (Fig. 5 A, arrowheads), indicating that the plasma membranes within the contact were bowed upward, away from the substratum, as the contact expanded (and hence out of focus for TIRF-M), but the contact remained anchored to the substratum at its edges. The proximity of E-cadherin–mediated adhesion to the substratum at the contact edges indicates that E-cadherin– and integrin-mediated adhesion sites are in very close spatial proximity to each other. Indeed, E-cadherin clusters marked by β-catenin staining at the edge of a cell–cell contact were closely associated with paxillin-positive integrin-mediated focal adhesions (Fig. 5, B–D). Although these two adhesion complexes form separate junctions, cortical actin bundles seem to be closely associated with both of them (Fig. 5, B–D).

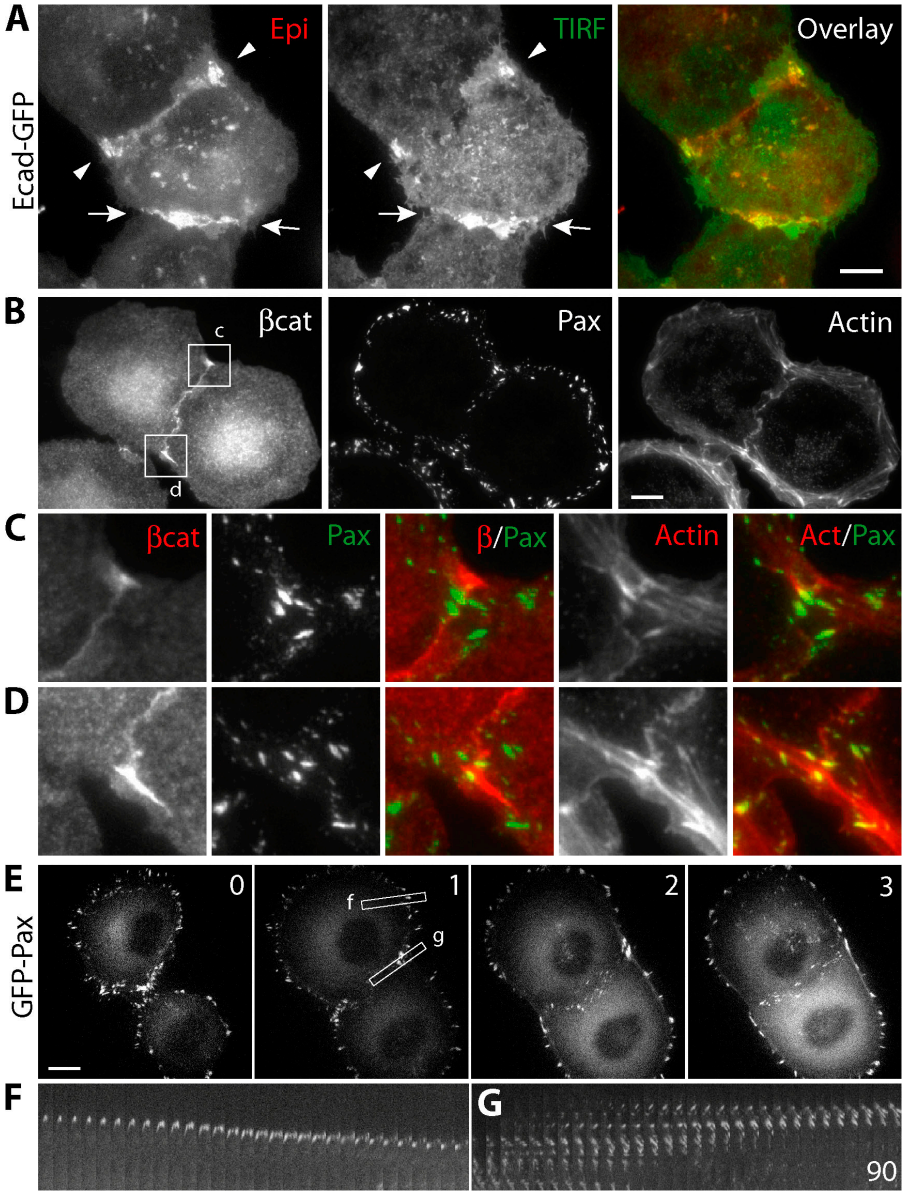

Figure 5. **Upstream signaling of RhoA activation.** (A) E-cadherin–GFP–expressing MDCK cells observed under epifluorescence or TIRF-M. (B) Colocalization of β-catenin, paxillin, and actin. (C and D) Close-up images of B. (E) GFP-paxillin–expressing MDCK cells making cell–cell contact. (F and G) Montages of GFP-paxillin at focal adhesion (F) and cell–cell contact (G). Bars, 10 μm.

We monitored focal adhesion formation during compaction of cell–cell contacts using GFP-paxillin as a maker for integrin-mediated adhesion. In contrast to the smooth, continuous movement of E-cadherin–GFP to the edge of the contact (Fig. 1 A), the translocation of GFP-paxillin to the edges of the expanding cell–cell contact occurred in steps (Fig. 5 E and Video 11, available at http://www.jcb.org/cgi/content/full/jcb.200701058/DC1), perhaps as a result of uncoordinated disassembly and assembly of focal adhesions. Indeed, closer inspection showed that new paxillin-positive focal adhesion formed at the edges of cell–cell contact and older ones disassembled from the center of the cell–cell contact, leaving behind only a few small and transient paxillin-containing focal adhesions (Fig. 5, E–G). Note that the reorganization and clustering of integrin-based focal adhesions at the edges of cell–cell contacts correlated spatially and temporally with localized activation of RhoA and myosin II by ROCK and MLCK.

Discussion

In this study, we used high-resolution live-cell imaging to show for the first time the distribution of active Rac1 and its downstream effectors the Arp2/3 complex and lamellipodia and active RhoA and its downstream effectors phosphomyosin II and actomyosin contraction during de novo contacts between stationary epithelial cells. Furthermore, we found that Rac1 and RhoA activation are under tight spatiotemporal control. Based on these novel findings, we define two stages of cell–cell adhesion driven initially by activation of Rac1 and lamellipodia, and then by activation of RhoA and actomyosin contraction (Fig. 6).

Initial adhesion appears to occur through opportunistic contacts between exploratory lamellipodia from opposing cells that result in the rapid accumulation of E-cadherin. At present, it is unclear whether E-cadherin accumulation is an active or passive process. Note that we did not detect synchronous actin accumulation with E-cadherin during de novo cell–cell adhesion, indicating that actin is not involved directly in initial E-cadherin reorganization. This is in agreement with binding studies with purified proteins showing that actin filaments do not bind directly to the cadherin–catenin complex (Drees et al., 2005; Yamada et al., 2005). Rapid diffusion of E-cadherin requires intrinsic plasma membrane activity that might mediate release of regional restrictions by local changes in actin organization.

The zone of E-cadherin accumulation spread outward as more contacts were formed by Rac1-induced lamellipodia at the periphery of the expanding contact (Fig. 4). Note, however, that active Rac1 was not detected within the E-cadherin zone, indicating that local Rac1 activity must be transient and down-regulated. Rac1 activation may be mediated directly by local activation of PI-3 kinase (Pece et al., 1999; Kovacs et al., 2002) and accumulation of phosphoinositides that recruit guanine exchange factors (Hordijk et al., 1997; Sander et al., 1998; Kovacs et al., 2002; Malliri et al., 2004), although we (Ehrlich et al., 2002) and others (Nakagawa et al., 2001; Betson et al., 2002) found that PI-3 kinase activity is not required for either Rac1 or E-cadherin accumulation at cell–cell contacts; further studies are needed to resolve this apparent conundrum.

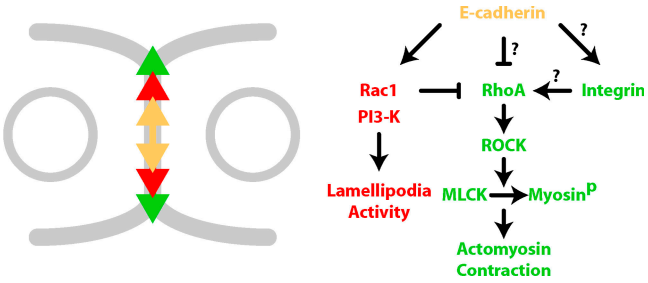

Figure 6. **Regulation of localized Rac1 and RhoA activation controls contact expansion.** (left) Series of signaling activation required for cell–cell contact expansion. Predicted zones of E-cadherin accumulation (yellow arrow), Rac1-induced lamellipodia protrusions (red arrow), and RhoA-induced actomyosin contraction (green arrow) coordinately induce, stabilize, and expand the cell–cell contact. (right) Positive and negative regulatory feedback loops controlling localized zones of E-cadherin accumulation, Rac1-induced lamellipodia protrusions, and RhoA-induced actomyosin contraction.

During this initial stage of cell–cell adhesion, we found that actin underwent a dramatic reorganization beneath the site of contact and E-cadherin accumulation; the cortical actin bundle found in single migratory cells appeared to dissolve beneath the site of contact, leaving the ends of the bundle bracketing the edges of the expanding contact and only faint actin staining at the contact. The reorganization of actin filaments at cell–cell contacts could be the result of concentrated lamellipodial activity in the immediate vicinity of newly formed cell–cell contacts (Fig. 4 B; Ehrlich et al., 2002) or the dramatic reorganization of integrin-based focal adhesion upon cell–cell adhesion (Fig. 5). In addition, we did not observe actin filaments directly inserting into the middle of cell–cell contacts at E-cadherin puncta at the ends of retracted thin filopodia close to the substratum or considerable amounts of actin polymerization around E-cadherin puncta, as reported in adhering keratinocytes (Vasioukhin et al., 2000; Vaezi et al., 2002). The difference in actin organization between simple epithelial (MDCK) cells and keratinocytes and may be due to the different cell types, although we note that we find actin bundles closely associated with the cadherin–catenin complex at the edges of the MDCK cell contacts, where integrin-based focal adhesions are also localized; it would be interesting to examine the distribution of integrin focal adhesions during cell–cell adhesion between keratinocytes.

The second stage of cell–cell adhesion involves active expansion of the contact that results in the formation of a strong cell–cell adhesion (Fig. 6). Expansion of adhesive contacts requires E-cadherin (Larue et al., 1994) and is an active process requiring localized actomyosin activation and contractility. Although previous studies reported the location of activated (phospho-) myosin II at cell–cell contacts and that disruption of regulatory pathways controlling activation of myosin II affects the maintenance and reformation of disrupted cell–cell contacts in confluent cell monolayers (Krendel and Bonder, 1999; Ivanov et al., 2004, 2005; Shewan et al., 2005), the present work is the first to analyze the spatiotemporal regulation of RhoA activity and actomyosin contractility during de novo cell–cell adhesion between pairs of cells.

We showed that active RhoA and phosphomyosin II were excluded from the center of the contact and restricted to the

cortical actin bundle in a zone at the outside edges of cell–cell contacts, where G-actin also incorporated. Several opposing signaling cascades may regulate the highly localized zone of RhoA-induced actomyosin activity at the margins of the contact edges (Fig. 6). RhoA activation and actomyosin contraction could be induced by local clustering of integrin-mediated adhesions at the edge of the cell–cell contact (DeMali et al., 2003). Alternatively, or in combination, RhoA activity could be suppressed in the center of the expanding contact by p120 catenin localized with cadherin along the contact (Anastasiadis and Reynolds, 2001; Wildenberg et al., 2006) or active Rac1 at the periphery of the E-cadherin zone (Sander et al., 1999). However, we have no direct evidence of these mechanisms at present, and further studies will be needed to test them directly.

Our studies indicate that actomyosin contractile forces were directed outward and backward from the cell–cell contact based on actin aster movements after CD-induced capping of actin filament barbed ends (Fig. 2, A–D). This activity would have the net effect of pulling the edges of the contacting membranes outward, to fully expand the contact to the width of the cells. Although the movement of cortical actin bundles at the edges of cell–cell contacts has been described and these cortical actin bundles are speculated as contractile bundles (Krendel and Bonder, 1999; Ehrlich et al., 2002), our results are the first to demonstrate the contraction and support previous speculation. This direction of contraction is opposite to that assumed to occur during the resealing of cell–cell contacts in cell monolayers (Krendel and Bonder, 1999; Ivanov et al., 2004, 2005; Zhang et al., 2005), indicating that different contractile mechanisms are involved in initial cell–cell adhesion and contacts between cells in established monolayers; however, the direction of contraction in cell monolayers has not be shown and should be reexamined and defined directly. At present, it is not clear how the barbed ends of the cortical actin bundle are anchored at the edges of the contact during de novo cell–cell adhesion, although high-resolution TIRF-M indicates that they are closely localized with E-cadherin (β-catenin) and integrin-based focal adhesions. The E-cadherin–catenin complex does not bind actin directly (Drees et al., 2005; Yamada et al., 2005), which indicates that at these sites actin may be anchored by integrin-based focal adhesions (DeMali et al., 2003), but further studies on actin linkages to integrins and cross talk with the E-cadherin–catenin complex are required to resolve the mechanisms involved.

In summary, we propose that two zones of Rho family GTPase activity are restricted to the edges of the cell–cell contact as it expands laterally and that they have different roles in initiating adhesive contacts (Rac1) and expanding and completing the contact (RhoA; Fig. 6). The zone of active Rac1 and its downstream effectors, the Arp2/3 complex and lamellipodia, is localized to de novo contacts between cells; these activities are transient and rapidly diminish as E-cadherin accumulates, but a new round of activation occurs at the periphery of the contacting membranes that would push the membranes together to initiate new E-cadherin adhesion. Diminished Rac1 activity, and hence membrane dynamics, in the newly formed cell–cell contact might allow the maintenance of weak trans-interactions between E-cadherin on opposing membranes. The zone of RhoA and its downstream effector actomyosin contractility is also restricted to the edges of the contact and is required to drive expansion and completion of cell–cell adhesion. Although we have not directly compared the distributions of active Rac1 and RhoA in the same cell, they appear different, with Rac1 localized over the tip of transient lamellipodia, whereas RhoA is localized continuously to the most distal sides of the edges of the expanding contact; we speculate, therefore, that the zone of RhoA activity may be on the outside of the Rac1 zone (Fig. 6). These sequential signaling zones comprising E-cadherin accumulation, Rac1-induced lamellipodia, and RhoA-induced actomyosin contraction coordinate the induction, initial stabilization, and expansion of the cell–cell contact (Fig. 6).

Materials and methods

Microscopy and image analysis

Formation of cell–cell contacts between stable MDCK cell lines expressing E-cadherin–GFP, GFP-actin, or GFP-paxillin was imaged with a custom confocal microscope (Adams et al., 1998) or the Marianas system (Intelligent Imaging, Inc.) equipped with a Xenon lamp (DG4 300W; Sutter Instrument) and camera (CoolSNAP HQ [Roper Scientific]; Yamada et al., 2005). The cells were imaged in DME media supplemented with 25 mM Hepes, and the temperature was kept at 37°C using a custom environmental enclosure. FITC-labeled actin (Cytoskeletal, Inc.) was added to saponin-permeabilized MDCK cells to locate polymerizing ends of actin filaments (Symons and Mitchison, 1991). GFP-actin turnover was measured with a FRAP module of Marianas system (Yamada et al., 2005). Images of myosin-stained MDCK cells were taken with an upright microscope (Axioplan; Carl Zeiss MicroImaging, Inc.) equipped with a mercury lamp; single band filter sets for FITC, Rhodamine, and Cy5; 100× Plan-NeoFluor 1.3 NA objective; and AxioCam M_r (Carl Zeiss MicroImaging, Inc.).

Raichu FRET probes for Rac1 (1026×) and RhoA (1298×) were variants of published probes that contained Venus instead of YFP and were gifts from M. Matsuda (Kyoto University, Kyoto, Japan). Using Lipofectamine 2000 (Invitrogen), MDCK cells were transiently transfected with the Raichu probes and imaged by Marianas system that configured with CFP/YFP filter set 86002v1(Chroma Technology). Pseudocolored ratio images were generated from images from CFP and FRET channels as described previously (Hodgson et al., 2006).

TIRF images were taken with a TIRF module on the Marianas system. The TIRF module consisted of a TIRF slider (Carl Zeiss MicroImaging, Inc.), 100× Plan-Fluor 1.45 NA objective, and 473- and 561-nm solid-state lasers (CrystaLaser).

All images were analyzed with ImageJ (http://rsb.info.nih.gov/ij/). In Fig. 3 F, The expansion velocities were calculated by dividing the change in the contact length by duration of drug treatment, and plotted as a function of normalized contact length (L[t]/Lf, where L[t] is contact length and Lf is final contact length). Because the expansion velocity depends on the maturation of cell–cell contact (Fig. 1 C), the mean velocity profile from Fig. 1 (D and E) is plotted as a reference (line).

Reagents

pEGFP-C1-paxillin and pEGFP-N1-Arp3 plasmids were gifts from C. Turner (State University of New York, Upstate Medical University, Syracuse, NY) and M. Welch (University of California, Berkeley, Berkeley, CA), respectively. Stable MDCK cell lines were generated as described previously (Yamada et al., 2005). Pharmacological agents were purchased from Sigma-Aldrich (CD and BDM) or Calbiochem (ML-7 and Y27632). Protein localizations in fixed cells were visualized with monoclonal myosin antibody (Beckman Coulter), polyclonal S19 phosphospecific myosin II antibody (generated by F. Matsumura, Rutgers University, New Brunswick, NJ), polyclonal anti–β-catenin (Hinck et al., 1994), and monoclonal anti-paxillin (BD Biosciences).

Online supplemental material

Video 1 is a time-lapse video of two E-cadherin–GFP–expressing MDCK cells making de novo cell–cell contact, shown in Fig. 1 A. Video 2 is a time-lapse video of two GFP-actin–expressing MDCK cells making de novo cell–cell contact, shown in Fig. 1 F. Video 3 is a time-lapse video of

GFP-actin–expressing MDCK cells treated with 0.5 μM CD, shown in Fig. 2 A. Video 4 is a time-lapse FRAP video of GFP-actin–expressing MDCK cells, shown in Fig. 2 F. Video 5 is a time-lapse video of GFP-actin–expressing MDCK cells treated with 25 μM ML-7 for 1 h, shown in Fig. 3 B. Video 6 is a time-lapse video of E-cadherin–GFP–expressing MDCK cells treated with 50 μM Y27632 for 1 h, shown in Fig. 3 D. Video 7 is a time-lapse video of GFP-actin–expressing MDCK cells treated with 50 μM Y27632 for 1 h, shown in Fig. 3 E. Video 8 is a time-lapse video of Raichu-Rac1–expressing MDCK cells, shown in Fig. 4 A. Video 9 is a time-lapse video of two Arp3-GFP–expressing MDCK cells making de novo cell–cell contact, shown in Fig. 4 B. Video 10 is a time-lapse video of Raichu-RhoA–expressing MDCK cells, shown in Fig. 4 D. Video 11 is a time-lapse video of two GFP-paxillin–expressing MDCK cells making de novo cell–cell contact, shown in Fig. 5 E. Online supplemental material is available at http://www.jcb.org/cgi/content/full/jcb.200701058/DC1.

We would like to thank Jason Ehrlich, who contributed early ideas and data to this work.

This work was support by a grant (GM35527) from the National Institutes of Health to W.J. Nelson.

Submitted: 10 January 2007
Accepted: 28 June 2007

References

Adams, C.L., Y.T. Chen, S.J. Smith, and W.J. Nelson. 1998. Mechanisms of epithelial cell-cell adhesion and cell compaction revealed by high-resolution tracking of E-cadherin-green fluorescent protein. *J. Cell Biol.* 142:1105–1119.

Anastasiadis, P.Z., and A.B. Reynolds. 2001. Regulation of Rho GTPases by p120-catenin. *Curr. Opin. Cell Biol.* 13:604–610.

Bertet, C., L. Sulak, and T. Lecuit. 2004. Myosin-dependent junction remodelling controls planar cell intercalation and axis elongation. *Nature.* 429:667–671.

Betson, M., E. Lozano, J. Zhang, and V.M. Braga. 2002. Rac activation upon cell-cell contact formation is dependent on signaling from the epidermal growth factor receptor. *J. Biol. Chem.* 277:36962–36969.

Braga, V.M., L.M. Machesky, A. Hall, and N.A. Hotchin. 1997. The small GTPases Rho and Rac are required for the establishment of cadherin-dependent cell-cell contacts. *J. Cell Biol.* 137:1421–1431.

Chen, X., and B.M. Gumbiner. 2006. Crosstalk between different adhesion molecules. *Curr. Opin. Cell Biol.* 18:572–578.

Conti, M.A., S. Even-Ram, C. Liu, K.M. Yamada, and R.S. Adelstein. 2004. Defects in cell adhesion and the visceral endoderm following ablation of nonmuscle myosin heavy chain II-A in mice. *J. Biol. Chem.* 279:41263–41266.

Costa, M., W. Raich, C. Agbunag, B. Leung, J. Hardin, and J.R. Priess. 1998. A putative catenin-cadherin system mediates morphogenesis of the *Caenorhabditis elegans* embryo. *J. Cell Biol.* 141:297–308.

Dawes-Hoang, R.E., K.M. Parmar, A.E. Christiansen, C.B. Phelps, A.H. Brand, and E.F. Wieschaus. 2005. *folded gastrulation*, cell shape change and the control of myosin localization. *Development.* 132:4165–4178.

DeMali, K.A., K. Wennerberg, and K. Burridge. 2003. Integrin signaling to the actin cytoskeleton. *Curr. Opin. Cell Biol.* 15:572–582.

Drees, F., S. Pokutta, S. Yamada, W.J. Nelson, and W.I. Weis. 2005. Alpha-catenin is a molecular switch that binds E-cadherin-beta-catenin and regulates actin-filament assembly. *Cell.* 123:903–915.

Ehrlich, J.S., M.D. Hansen, and W.J. Nelson. 2002. Spatio-temporal regulation of Rac1 localization and lamellipodia dynamics during epithelial cell-cell adhesion. *Dev. Cell.* 3:259–270.

Etienne-Manneville, S., and A. Hall. 2002. Rho GTPases in cell biology. *Nature.* 420:629–635.

Gumbiner, B.M. 2005. Regulation of cadherin-mediated adhesion in morphogenesis. *Nat. Rev. Mol. Cell Biol.* 6:622–634.

Hayashi, T., and R.W. Carthew. 2004. Surface mechanics mediate pattern formation in the developing retina. *Nature.* 431:647–652.

Hinck, L., W.J. Nelson, and J. Papkoff. 1994. Wnt-1 modulates cell-cell adhesion in mammalian cells by stabilizing beta-catenin binding to the cell adhesion protein cadherin. *J. Cell Biol.* 124:729–741.

Hodgson, L., P. Nalbant, F. Shen, and K. Hahn. 2006. Imaging and photobleach correction of Mero-CBD, sensor of endogenous Cdc42 activation. *Methods Enzymol.* 406:140–156.

Hordijk, P.L., J.P. ten Klooster, R.A. van der Kammen, F. Michiels, L.C. Oomen, and J.G. Collard. 1997. Inhibition of invasion of epithelial cells by Tiam1-Rac signaling. *Science.* 278:1464–1466.

Itoh, R.E., K. Kurokawa, Y. Ohba, H. Yoshizaki, N. Mochizuki, and M. Matsuda. 2002. Activation of rac and cdc42 video imaged by fluorescent resonance energy transfer-based single-molecule probes in the membrane of living cells. *Mol. Cell. Biol.* 22:6582–6591.

Ivanov, A.I., I.C. McCall, C.A. Parkos, and A. Nusrat. 2004. Role for actin filament turnover and a myosin II motor in cytoskeleton-driven disassembly of the epithelial apical junctional complex. *Mol. Biol. Cell.* 15:2639–2651.

Ivanov, A.I., D. Hunt, M. Utech, A. Nusrat, and C.A. Parkos. 2005. Differential roles for actin polymerization and a myosin II motor in assembly of the epithelial apical junctional complex. *Mol. Biol. Cell.* 16:2636–2650.

Jou, T.S., and W.J. Nelson. 1998. Effects of regulated expression of mutant RhoA and Rac1 small GTPases on the development of epithelial (MDCK) cell polarity. *J. Cell Biol.* 142:85–100.

Kovacs, E.M., R.G. Ali, A.J. McCormack, and A.S. Yap. 2002. E-cadherin homophilic ligation directly signals through Rac and phosphatidylinositol 3-kinase to regulate adhesive contacts. *J. Biol. Chem.* 277:6708–6718.

Krendel, M.F., and E.M. Bonder. 1999. Analysis of actin filament bundle dynamics during contact formation in live epithelial cells. *Cell Motil. Cytoskeleton.* 43:296–309.

Krendel, M., N.A. Gloushankova, E.M. Bonder, H.H. Feder, J.M. Vasiliev, and I.M. Gelfand. 1999. Myosin-dependent contractile activity of the actin cytoskeleton modulates the spatial organization of cell-cell contacts in cultured epitheliocytes. *Proc. Natl. Acad. Sci. USA.* 96:9666–9670.

Larue, L., M. Ohsugi, J. Hirchenhain, and R. Kemler. 1994. E-cadherin null mutant embryos fail to form a trophectoderm epithelium. *Proc. Natl. Acad. Sci. USA.* 91:8263–8267.

Lee, C.H., and B.M. Gumbiner. 1995. Disruption of gastrulation movements in *Xenopus* by a dominant-negative mutant for C-cadherin. *Dev. Biol.* 171:363–373.

Malliri, A., S. van Es, S. Huveneers, and J.G. Collard. 2004. The Rac exchange factor Tiam1 is required for the establishment and maintenance of cadherin-based adhesions. *J. Biol. Chem.* 279:30092–30098.

Matsumura, F., S. Ono, Y. Yamakita, G. Totsukawa, and S. Yamashiro. 1998. Specific localization of serine 19 phosphorylated myosin II during cell locomotion and mitosis of cultured cells. *J. Cell Biol.* 140:119–129.

Nakagawa, M., M. Fukata, M. Yamaga, N. Itoh, and K. Kaibuchi. 2001. Recruitment and activation of Rac1 by the formation of E-cadherin-mediated cell-cell adhesion sites. *J. Cell Sci.* 114:1829–1838.

Noren, N.K., C.M. Niessen, B.M. Gumbiner, and K. Burridge. 2001. Cadherin engagement regulates Rho family GTPases. *J. Biol. Chem.* 276:33305–33308.

Pece, S., M. Chiariello, C. Murga, and J.S. Gutkind. 1999. Activation of the protein kinase Akt/PKB by the formation of E-cadherin-mediated cell-cell junctions. Evidence for the association of phosphatidylinositol 3-kinase with the E-cadherin adhesion complex. *J. Biol. Chem.* 274:19347–19351.

Pertz, O., L. Hodgson, R.L. Klemke, and K.M. Hahn. 2006. Spatiotemporal dynamics of RhoA activity in migrating cells. *Nature.* 440:1069–1072.

Ren, X.D., W.B. Kiosses, and M.A. Schwartz. 1999. Regulation of the small GTP-binding protein Rho by cell adhesion and the cytoskeleton. *EMBO J.* 18:578–585.

Sander, E.E., S. van Delft, J.P. ten Klooster, T. Reid, R.A. van der Kammen, F. Michiels, and J.G. Collard. 1998. Matrix-dependent Tiam1/Rac signaling in epithelial cells promotes either cell-cell adhesion or cell migration and is regulated by phosphatidylinositol 3-kinase. *J. Cell Biol.* 143:1385–1398.

Sander, E.E., J.P. ten Klooster, S. van Delft, R.A. van der Kammen, and J.G. Collard. 1999. Rac downregulates Rho activity: reciprocal balance between both GTPases determines cellular morphology and migratory behavior. *J. Cell Biol.* 147:1009–1022.

Shewan, A.M., M. Maddugoda, A. Kraemer, S.J. Stehbens, S. Verma, E.M. Kovacs, and A.S. Yap. 2005. Myosin 2 is a key Rho kinase target necessary for the local concentration of E-cadherin at cell-cell contacts. *Mol. Biol. Cell.* 16:4531–4542.

Symons, M.H., and T.J. Mitchison. 1991. Control of actin polymerization in live and permeabilized fibroblasts. *J. Cell Biol.* 114:503–513.

Takaishi, K., T. Sasaki, H. Kotani, H. Nishioka, and Y. Takai. 1997. Regulation of cell-cell adhesion by rac and rho small G proteins in MDCK cells. *J. Cell Biol.* 139:1047–1059.

Takeichi, M. 1995. Morphogenetic roles of classic cadherins. *Curr. Opin. Cell Biol.* 7:619–627.

Vaezi, A., C. Bauer, V. Vasioukhin, and E. Fuchs. 2002. Actin cable dynamics and Rho/Rock orchestrate a polarized cytoskeletal architecture in the early steps of assembling a stratified epithelium. *Dev. Cell.* 3:367–381.

Vasioukhin, V., C. Bauer, M. Yin, and E. Fuchs. 2000. Directed actin polymerization is the driving force for epithelial cell-cell adhesion. *Cell.* 100:209–219.

Verkhovsky, A.B., T.M. Svitkina, and G.G. Borisy. 1997. Polarity sorting of actin filaments in cytochalasin-treated fibroblasts. *J. Cell Sci.* 110:1693–1704.

Vestweber, D., and R. Kemler. 1985. Identification of a putative cell adhesion domain of uvomorulin. *EMBO J.* 4:3393–3398.

Welch, M.D., A.H. DePace, S. Verma, A. Iwamatsu, and T.J. Mitchison. 1997. The human Arp2/3 complex is composed of evolutionarily conserved subunits and is localized to cellular regions of dynamic actin filament assembly. *J. Cell Biol.* 138:375–384.

Wildenberg, G.A., M.R. Dohn, R.H. Carnahan, M.A. Davis, N.A. Lobdell, J. Settleman, and A.B. Reynolds. 2006. p120-catenin and p190RhoGAP regulate cell-cell adhesion by coordinating antagonism between Rac and Rho. *Cell.* 127:1027–1039.

Yamada, S., S. Pokutta, F. Drees, W.I. Weis, and W.J. Nelson. 2005. Deconstructing the cadherin-catenin-actin complex. *Cell.* 123:889–901.

Yoshizaki, H., Y. Ohba, K. Kurokawa, R.E. Itoh, T. Nakamura, N. Mochizuki, K. Nagashima, and M. Matsuda. 2003. Activity of Rho-family GTPases during cell division as visualized with FRET-based probes. *J. Cell Biol.* 162:223–232.

Zallen, J.A., and E. Wieschaus. 2004. Patterned gene expression directs bipolar planar polarity in *Drosophila*. *Dev. Cell.* 6:343–355.

Zhang, J., M. Betson, J. Erasmus, K. Zeikos, M. Bailly, L.P. Cramer, and V.M. Braga. 2005. Actin at cell-cell junctions is composed of two dynamic and functional populations. *J. Cell Sci.* 118:5549–5562.